Author's personal copy

Journal of Neuroscience Methods 232 (2014) 102–109

Contents lists available at ScienceDirect

Journal of Neuroscience Methods

journal homepage: www.elsevier.com/locate/jneumeth

Computational Neuroscience

Nonlinear analysis of saccade speed fluctuations during combined action and perception tasks

C. Stan[a], C. Astefanoaei[b], E. Pretegiani[c], L. Optican[d], D. Creanga[b,*], A. Rufa[c], C.P. Cristescu[a]

[a] Department of Physics, Politehnica University of Bucharest, 313 Spl. Independentei, RO 060042, Romania
[b] Physics Department, University Alexandru Ioan Cuza, 11 Blvd. Carol I., Iasi, Romania
[c] Eye-tracking & Visual Application Lab EVALab, Department of Medicine Surgery and Neuroscience, University of Siena, Siena 53100, Italy
[d] Laboratory of Sensorimotor Research, IRP, National Eye Institute, DHHS, Bethesda, MD 20892, USA

HIGHLIGHTS

- Saccadic peak speed fluctuations are multifractal.
- Saccade multifractality strength differs in simple decision and dual decision task.
- Similar results for Lempel–Ziv analysis show different complexity measures.
- Multifractal parameter proposed for action–perception interaction in visual process.

ARTICLE INFO

Article history:
Received 20 February 2014
Received in revised form 9 May 2014
Accepted 12 May 2014

PACS:
87.10.Mn
87.18.Tt
87.19.L–

Keywords:
Saccade speed peak
Action–perception task
Multifractal properties
Lempel–Ziv complexity

ABSTRACT

Background: Saccades are rapid eye movements used to gather information about a scene which requires both action and perception. These are usually studied separately, so that how perception influences action is not well understood. In a dual task, where the subject looks at a target and reports a decision, subtle changes in the saccades might be caused by action–perception interactions. Studying saccades might provide insight into how brain pathways for action and for perception interact.
New method: We applied two complementary methods, multifractal detrended fluctuation analysis and Lempel–Ziv complexity index to eye peak speed recorded in two experiments, a pure action task and a combined action–perception task.
Results: Multifractality strength is significantly different in the two experiments, showing smaller values for dual decision task saccades compared to simple-task saccades. The normalized Lempel–Ziv complexity index behaves similarly i.e. is significantly smaller in the decision saccade task than in the simple task.
Comparison with existing methods: Compared to the usual statistical and linear approaches, these analyses emphasize the character of the dynamics involved in the fluctuations and offer a sensitive tool for quantitative evaluation of the multifractal features and of the complexity measure in the saccades peak speeds when different brain circuits are involved.
Conclusion: Our results prove that the peak speed fluctuations have multifractal characteristics with lower magnitude for the multifractality strength and for the complexity index when two neural pathways are simultaneously activated, demonstrating the nonlinear interaction in the brain pathways for action and perception.

© 2014 Elsevier B.V. All rights reserved.

1. Introduction

Saccades are rapid eye movements initiated by activation of neurons widely distributed across the cerebrum, the cerebellum, and the brain stem. Study of saccades is popular since they can intermediate ways of studying motor control, cognition and memory. From saccade analysis it has been possible to identify distinct populations of neurons from brainstem to cerebral cortex that

* Corresponding author at: Physics Department, University Alexandru Ioan Cuza, 11 Blvd. Carol I., Iasi 700506, Romania. Tel.: +40 232201180; fax: +40 232201150.
E-mail addresses: cstan@physics.pub.ro (C. Stan), corina_astefanoaei@yahoo.com (C. Astefanoaei), elena.pretegiani@nih.gov (E. Pretegiani), lmo@lsr.nei.nih.gov (L. Optican), dorina.creanga@gmail.com (D. Creanga), rufa@unisi.it (A. Rufa), cpcris@physics.pub.ro (C.P. Cristescu).

http://dx.doi.org/10.1016/j.jneumeth.2014.05.010
0165-0270/© 2014 Elsevier B.V. All rights reserved.

Author's personal copy

contribute to behaviors ranging from reflexive glances to memorized sequences of saccades during learned tasks (Leigh and Kennard, 2004). Saccade investigations are used both by neurologists and neuroscientists in order to develop models and schemes of circuit equivalence of different regions of the brain associated with specific behaviors (Wong and Shelhamer, 2013; Daye et al., 2013).

Gathering information about a scene requires both action and perception. However, in most experiments these are usually studied separately, so that how perception influences action is not well understood. In a dual task, where the subject looks at a target and reports a decision, subtle changes in the saccades might be caused by action/perception interactions.

New evidence of multiplicative interactions in cognitive performance suggests that cognitive processes at different scales of time and space are interdependent and interaction-dominant (Zheng et al., 2005; Ihlen and Vereijken, 2010; Kelty-Stephen and Mirman, 2013). In this context, recent development of nonlinear methods such as multifractal analysis or Lempel–Ziv complexity index can give new framework for analyzing and understanding the complex dynamics of different neuronal pathways involved in perception and action and also in the perception–action coupling. The neural circuits are regulated by complex dynamics that incorporate memory of past events, and the strength of this memory can be estimated by the Hurst exponent. Moreover, the degree of randomness in the dynamics of perception–action coupling is properly described by the algorithmic complexity function expressed by Lempel–Ziv metric.

Fractal and multifractal analysis has been extensively used in studies of the fluctuations in biological phenomena (Stan et al., 2013), neuroscience (Zheng et al., 2005), linguistic analysis (Ausloos, 2012; Suckling et al., 2008), EEG pattern (Wang et al., 2003; Dutta et al., 2014; Kumar et al., 2013), eye movement (Shelhamer, 2005; Ihlen and Vereijken, 2010; Schmeisser et al., 2001; Kelty-Stephen and Nixon, 2013; Astefanoaei et al., 2013).

Various implementations of the method use multifractal detrended fluctuation analysis (MF-DFA) (Kantelhardt et al., 2002), continuous wavelet transform modulus maxima (Muzy et al., 1993), structure function and singular measures formalisms (Yu et al., 2003; Tessier et al., 1996). Multifractal analysis by the MF-DFA method of neural activity was used by some authors (Kumar et al., 2013), who reported that optogenetically stimulated neural firings are consistent with a multifractal process. This computational procedure has shown that the generalized Hurst exponent exhibited dramatic changes that could differentiate neural activities during control phases and phases with chemically induced pain. According to other authors (Dojnow and Vitanov, 2008), numerical analysis with the Hurst generalized exponent of relatively short EEC data series revealed multifractal features in underlying processes; the authors claimed to develop a putative computational tool in the investigation of brain subsystems based on the neural activity mapping during cognitive task performance.

Multifractal characteristics in measured eye-tracking fluctuations were reported (Coey et al., 2012) with a focus on the influence of the eye-tracking instrument on the structure of measured signal variability. Their results provided evidence that the fractal structure in the variability of eye-movement data is not an artifact of the data recording device but an intrinsic behavioral trend in the subjects. It seems that whenever a subject executes saccades between fixation point and target, there are variations in eye position. Such trial-to-trial variation has usually been treated as purely experimental noise and cancelled out by averaging and smoothing over trials. Therefore fluctuations detected either in the eye movement (Coey et al., 2012) or fixation (Kelty-Stephen and Mirman, 2013) are still poorly explained.

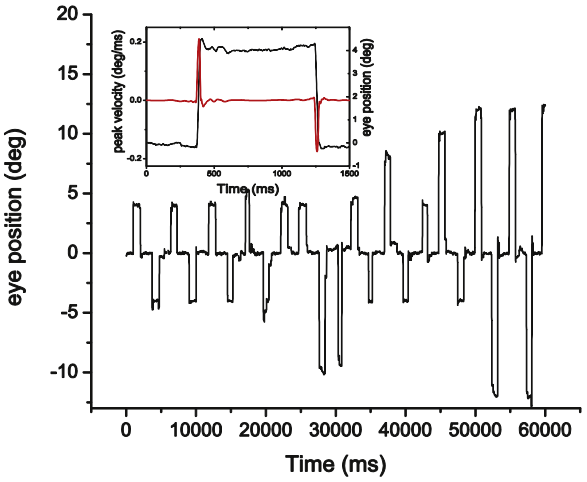

Fig. 1. Representation of eye saccadic response displayed for 60 s recording. Inset is an illustration of peak velocity computation.

The complexity of discrete-time signals of biomedical interest has also been investigated using the Lempel–Ziv analysis (Lempel and Ziv, 1976), proposed for the evaluation of the randomness in finite sequences of data as an extension of the algorithmic complexity function (Kolmogorov, 1965; Chaitin, 1966). The L–Z measure of complexity is related to the number of distinct substrings (i.e. patterns) and the rate of their occurrence along a given data sequence (Aboy et al., 2006). This measure has been used in biomedical research, such as in genomic sequence investigations for revealing patterns in DNA structure, in estimation of neural firing entropy and for describing neuronal responses induced in the visual cortex by different types of stimulation (Stan et al., 2013; Szczepaski et al., 2003; Amigo et al., 2004). The advantages of this method over correlation entropy from chaos theory were discussed by Hu et al. (2006), who studied the possibility of epileptic seizure detection from EEG data.

In the present study, we focus on the application of two complementary methods, multifractal analysis and the L–Z complexity to the identification of the nonlinear characteristics of saccadic visual exploration, by analyzing fluctuations in the peak speed eye movement during a simple action task and a dual action–perception task.

2. Methods

2.1. Data recording

Saccadic eye movements (Fig. 1) were recorded with a video-based eye tracker (iViewX Hi Speed, SMI) consisting in temporal series of angular shift values. Subjects' right eye movements were recorded at a sample rate of 1000 Hz. Only horizontal eye movements were analyzed. The subjects were nine healthy, adult volunteers who took part in an experimental research developed in the Laboratory of Sensorimotor Research, at National Eye Institute (NEI), National Institutes of Health (NIH), USA. The experiments conformed to the human subjects guidelines of the NIH for human subject research, and with the Declaration of Helsinki, were approved by the NEI institutional review board, and the subjects provided written, informed consent. Drug and alcohol influence was excluded in all subjects. Neuro-ophthalmological examination was carried out before the experimental saccadic study and no clinical, neurological pathologies nor visual impairment was found, except very mild refractive error in some cases (during the experiment the subjects worked without glasses). Visual stimuli were two

Author's personal copy

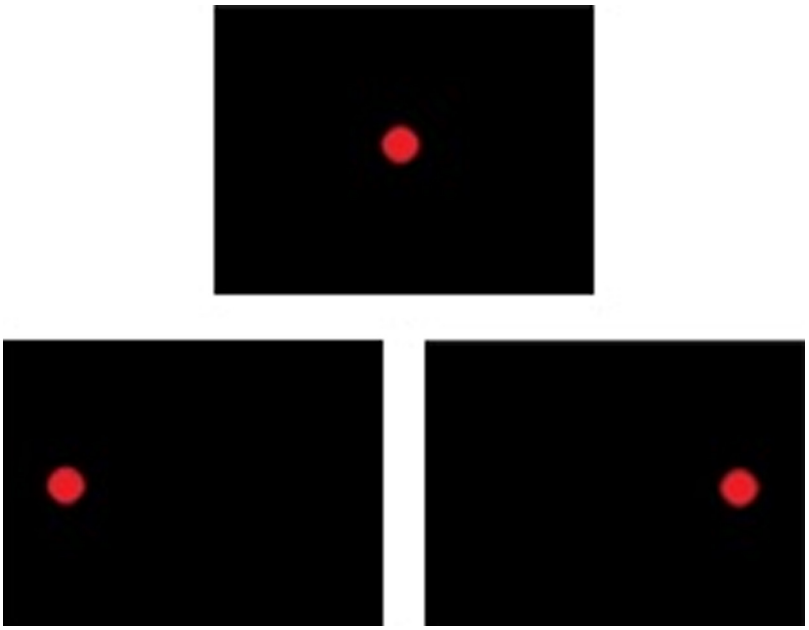

Fig. 2. Visual stimuli presentation.

red laser spots (diameter of 3 mm, visual angle of 0.16°) projected onto a screen placed 105 cm in front of the subject's eyes.

One of the spots was presented in the centre of the screen acting as fixation point (Fig. 2). The other spot (the target) could be moved horizontally to the left or right of the central fixation point by mirror galvanometers (General Scanning, Inc., Watertown, CT; controller model 310-140362, motor model 3008001). The recordings took place in a dimly illuminated room with screen luminance of 0.009 cd/m^2 as measured with a Konica Minolta LS-100 luminance meter.

As the light spots were bright (fixation point 46.35 cd/m^2 and target 46.69 cd/m^2), and latency, but not accuracy was measured, no vision correction was needed. A real-time data acquisition and control system (REX, version 8.0) was used to carry out the measurements (Hays et al., 1982). The experiment was designed as follows: first, the central fixation point came on. The duration of the fixation point was randomly chosen from the set: 1600, 1700, 1800, 1900, 2000 ms. Then a target appeared at an eccentric location (4, 6, 8, 10 or 12°, to the left or right of the central fixation point).

Duration of the target presence was randomly chosen from the set: (1000, 1050, 1100, 1150, 1200 ms). The appearance of the target could follow the offset of the fixation point, so that for a moment there were no visual stimuli on the screen (gap condition), or it could precede the offset of the fixation point, so that for a short time there were two visual stimuli on the screen (overlap condition).

The subjects took part in two experiments: a simple saccadic task (SST) and a dual saccade-decision task (DST). In the SST recording session, according to the experimental protocol proposed by Saslow (1967), the subject was instructed to look at the fixation point, but as soon as an eccentric target appeared, to execute a saccade to the target and then maintain fixation on the target until its disappearance. Subject returned to the fixation point when it reappeared. In the DST, the subjects were instructed to execute saccades as before, but after looking at the target they were requested to push one of two buttons, indicating whether they saw a gap between, or an overlap of the two lights. Each session took about 25–30 min, with a 1–2 min break after every 5–6 min of recording. Lubricating eye drops were applied if requested.

2.2. Data processing

Data series collected from 9 subjects were processed and studied with mathematical algorithms for multifractal analysis and L–Z complexity analysis. The investigation focuses on the peak speed fluctuations of eye movement in two situations: SST and DST task.

The peak speed sequences were constructed after the identification of each saccade individually. Artefacts, such as blinks or saturation of the eye tracker signal, were eliminated in a first stage processing. After numerical differentiation of the recorded data sets of the eye movement position (Fig. 1) we consider only the peak speed computed from the smoothing of the original peak profile. Inset of Fig. 1 is an illustration of a peak velocity computation (scale on the left side) for a saccadic movement to the target of 4° and back (scale on the right side). Only peaks separated by at least 1000 ms (the minimal target duration according to the experimental design) were selected.

The peak speed time series were constructed in strict agreement with the succession of stimuli. Trials with peak speed values outside the normal range (less than 25°/s or more than 800°/s) were excluded. We consider the peak velocity of the saccadic eye movement in absolute value, resulting in series of similar size (about 1000 points) for all subjects and for both experimental procedure.

3. Results and discussion

We present the results obtained from the application of two types of data analysis: multifractal analysis based on MF-DFA method and complexity analysis based on Lempel–Ziv complexity index.

Typical sequences of time series for the same subject in both tasks are shown in Fig. 3.

3.1. Multifractal detrended fluctuation analysis

Multifractal analysis allows the computation of the dependence of the generalized Hurst exponent on the moment order, of the singularity spectrum and of the fractal dimensions of fluctuations. To investigate the fractal characteristics of the saccades

Author's personal copy

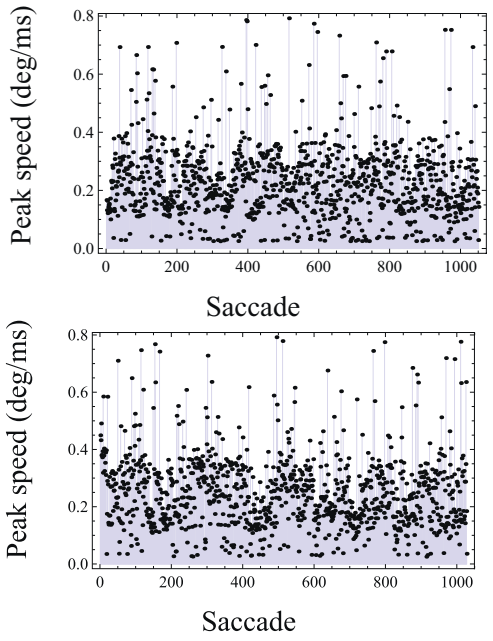

Fig. 3. Peak speed series of eye movement versus the index of consecutive saccades (a) SST and (b) DST.

peak speed, we use the multifractal analysis formalism according to Kantelhardt et al. (2002).

For a time-series of N data, the "profile" is defined as:

$$Y(j) = \sum_{i=1}^{j} (y_i - \langle y \rangle); \quad j = 1, 2, \ldots, N \tag{1}$$

where $\langle y \rangle$ is the mean value of the analyzed series. The new series $Y(j)$ is then divided into 2 N_s non-overlapping segments ($N_s = \mathrm{Int}(N/s)$) of length s, starting from the beginning to the end and in reverse. These series can be characterized by the variance:

$$F^2(s, \nu) = \frac{1}{s} \sum_{k=1}^{s} (Y_\nu(k) - \hat{Y}_\nu(k)); \quad \nu = 1, 2, \ldots, N_s \tag{2}$$

and by a q-order fluctuation function:

$$F(q, s) = \left\{ \frac{1}{2N_s} \sum_{\nu=1}^{2N_s} [F^2(s, \nu)]^{q/2} \right\}^{1/q}, \tag{3}$$

where $Y_\nu(k)$ represents the fragment of the series corresponding to the segment ν and $\hat{Y}_\nu(k)$, $k = 1, \ldots, s$ is its best polynomial fit on the specific segment ν. For a statistically self-affine series, the dependence of the fluctuation function on the size s of the segment is expected to be power law type:

$$F(q, s) \approx s^{h(q)} \tag{4}$$

where $h(q)$ is known as generalized Hurst exponent for the profile series and is computed from the log–log plot of the fluctuation function versus s as the slope in the scaling region. In the present study, the MF-DFA is used to compute the generalized Hurst exponent for a certain range of values of the q-order fluctuation functions (Kantelhardt et al., 2002; Ihlen, 2012).

Important elements in the multifractal analysis are the scaling interval, i.e. the interval of linear dependence between the fluctuation function and the length of the segment s in the log–log plot, and the interval of the values for q-order fluctuation. In many applications to analysis of empirical data, the values of these parameters are key issues for understanding the physical mechanisms involved

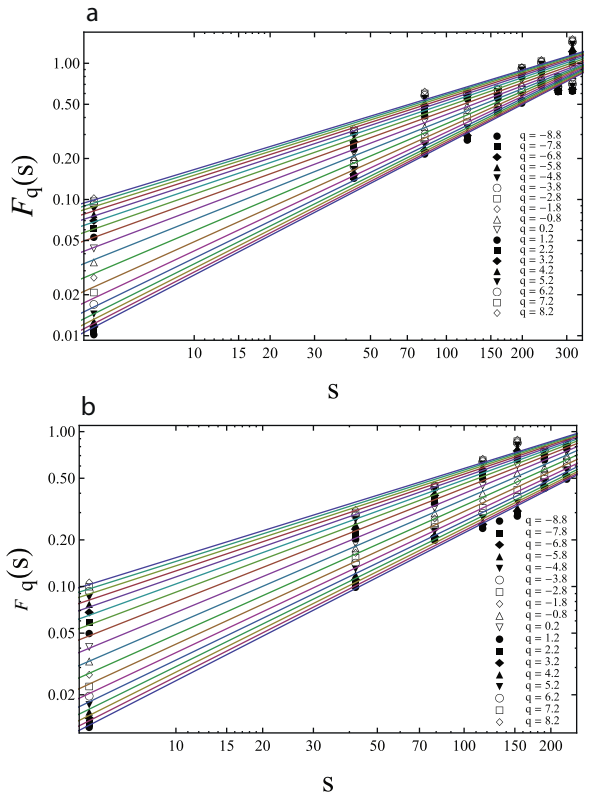

Fig. 4. Illustration of the log–log plot dependence for the fluctuation function $F(q,s)$ versus s corresponding to the time-series from Fig. 3: (a) SST and (b) DST.

in scaling phenomena. In the case of measured data, the true source and true trends are often unknown, therefore there are no universal rules for finding the optimum values for these parameters and also not enough literature illustrating the limitation rules. Since the characteristics of the experimental data are oftentimes far from the well-known properties of the simulated processes, a common practice is to check the goodness of the fit for the polynomial chosen in MFDFA for each of the q-order fluctuation function (Ihlen, 2012).

In order to satisfy the accepted condition of MF-DFA for the length of the non-overlapping segments (Kantelhardt et al., 2002), we decided to use $s = 250$ as maximum length. For all analyzed cases the log–log plot of the dependence for the fluctuation function $F(q,s)$ on s is linear for all considered values of q between −10 and 10, with a coefficient of determination ($r^2 > 0.95$), showing that long range correlations for individual series exists up to this maximum value of s (Fig. 4).

The generalized Hurst exponent for each moment order, $h(q)$ is a measure for the correlation of the fluctuations related to q, i.e. in small fluctuations range for $q < 0$ and large fluctuations range for $q > 0$. The Hurst exponent computed for $q = 2$ is considered as the main Hurst exponent. If $h(2) > 0.5$ the correlations in the time series are persistent, i.e. an increment has higher probability of being followed by another increment. If $h(2) < 0.5$ the correlations in the time series are anti-persistent, i.e. an increment has more chances of being followed by a decrement and vice-versa. If $h(2) = 0.5$ only short range correlations or no correlations exist as in the case of white Gaussian noise.

For any value of q, the meaning of $h(q)$ is the same as that of $h(2)$. Monofractal time series are characterized by $h(q)$ independent of q while for multifractal time series $h(q)$ is a non-linearly decreasing function of q.

Theoretically, the multifractality strength is measured by the difference of the values of $h(q)$ for the limits of the range of orders

Author's personal copy

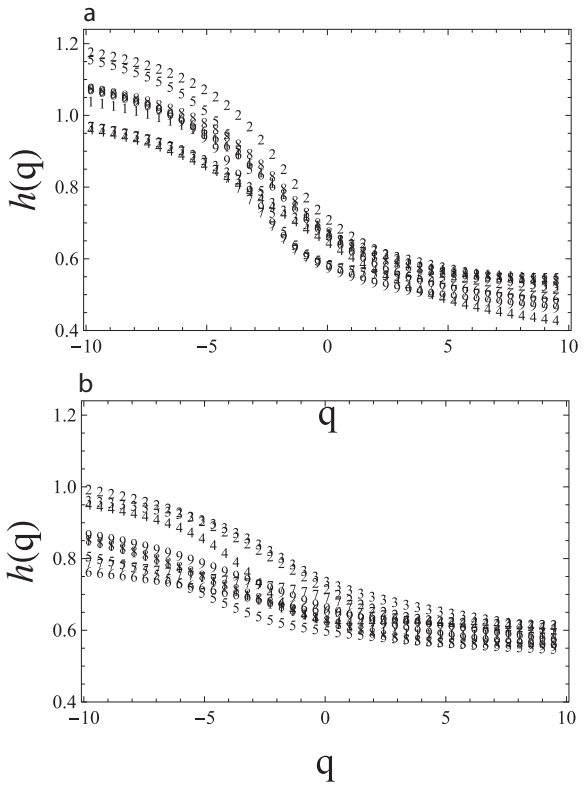

Fig. 5. Generalized Hurst exponent spectra: (a) SST and (b) DST.

i.e. $h(-\infty)-h(+\infty)$. As this is very difficult to estimate for real life (experimental) time series we use instead:

$$\Delta h = h(q_{\min}) - h(q_{\max}) \quad (5)$$

with $q_{\min}$ and $q_{\max}$ the extreme values of q considered in our computation ($q_{\min} = -10$ and $q_{\max} = +10$). The larger the multifractality strength, the larger the difference between the scaling characteristics of small and large fluctuations in a time-series.

Fig. 5 shows the generalized Hurst exponent spectra for the analyzed subjects (marked with corresponding digits) in the two experimental situations.

According to Fig. 5, multifractality is present in both experiments, $h(q)$ dependence showing nonlinear decreasing. The range of $h(q)$ variation across the subjects is larger in the SST experiment (Fig. 5a), with $h(q_{\min})$ ranging from 0.95 to 1.2 and $h(q_{\max})$ ranging from 0.41 to 0.55, compared to the DST experiment (Fig. 5b); where $h(q_{\min})$ ranges from 0.75 to 1.00 and $h(q_{\max})$ ranges from 0.54 to 0.63. One could say that in the second experiment, when the dual-task involves a higher cognitive load, $h(q)$ tends to depend less on q.

Observing the differences in Fig. 5 between SST and DST, we may argue that the additional cognitive load significantly reduces multifractality. The results provided by the generalized Hurst exponent are described by the mean and standard deviation of the average across the nine analyses: $\{h(q_{\max}) = 0.50 \pm 0.04$; $h(q_{\min}) = 1.05 \pm 0.08\}$ for SST and $\{h(q_{\max}) = 0.58 \pm 0.02$; $h(q_{\min}) = 0.87 \pm 0.08\}$ for DST. We notice that while for small fluctuations ($q < 0$) the change in $h(q)$ is qualitatively insignificant (describes positive correlation in both cases), for large fluctuations ($q > 0$), the change in $h(q)$ shows a transition from no correlation in SST to positive correlation in DST. One could conclude that the narrower range of the average Hurst exponent in DST compared to SST is the result of the subject's focusing on a more difficult task, the combined action–perception task.

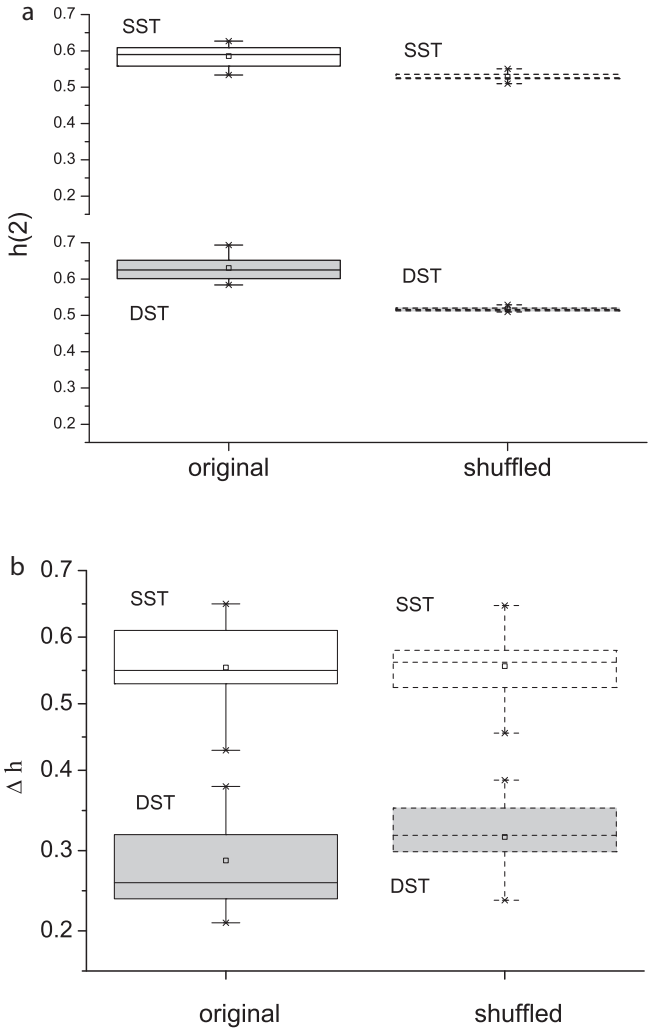

Fig. 6. Box chart representation of: (a) Hurst main exponent and (b) multifractal strength for initial and shuffled data in SST and DST.

To get a deeper insight into the origin of multifractality in the two saccadic data types, the shuffling procedure was applied. According to Telesca et al. (2004), multifractality types in time series could be describe as:

- type (i), due to a broad probability density function;
- type (ii), due to different long-range correlations for small and large fluctuations.

For a data series whose probability mass distribution (p.m.d.) is regular with finite moments and uncorrelated, multifractality is mostly of the first type while for correlated series the multifractal character is of the second type. Discerning between the two types can be obtained by performing a shuffling of the series – randomly rearranging the samples. This procedure clearly destroys the correlations while the p.m.d. is not affected.

We performed the shuffling process for every saccadic data, by generating 20 shuffled replicas and then computing a generic shuffled series as an average over the 20 shufflings.

Box plot representation of data series was applied to get a visual comparison of two distributions as well as statistical parameters allowing numerical comparison. The shuffled series show residual multifractality (Fig. 6), that can be only a consequence of the power-law type distribution.

Author's personal copy

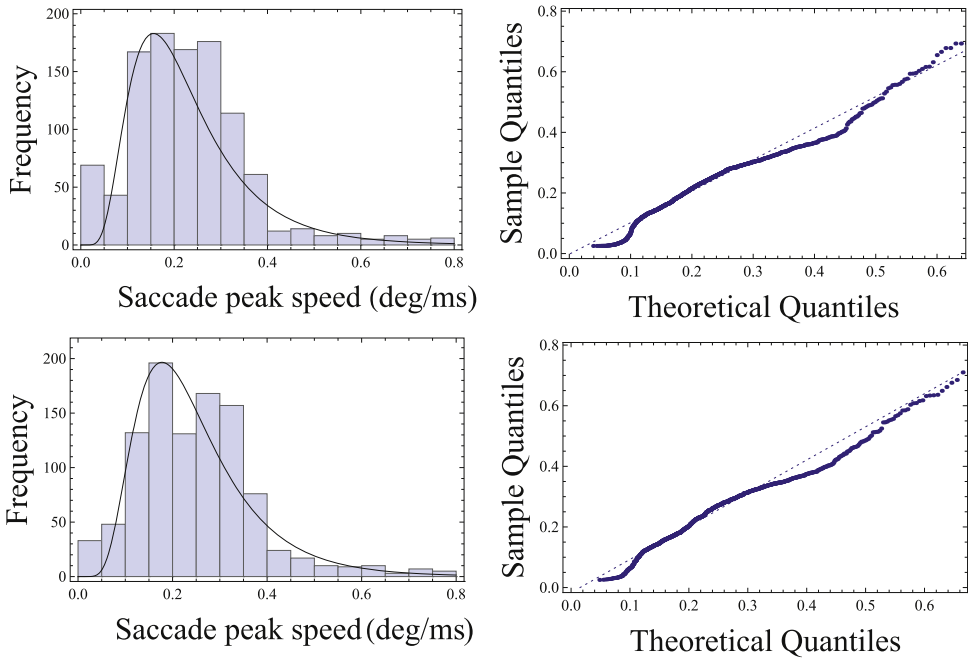

Fig. 7. Histograms for a particular subject and the log-normal fitting: (a) SST; (c) DST; and the goodness of the fit shown by quantile plots (b) and (d), respectively.

Box plot representations of the Hurst main exponent for the initial and shuffled data (Fig. 6a) show some differences between SST and DST data. The median value moved non-significantly from 0.586 for SST to 0.630 for DST while the box size remained approximately the same (0.035). Consequently, fluctuations described by the main Hurst exponent keep a low level of persistence, close to the random case (with $h(2) \approx 0.5$), after adding the decision task to the saccade only task.

As expected, the shuffling procedure led to a significant decrease of $h(2)_{shuf}$ in both studied conditions (with $p < 0.001$ for SST and $p < 0.00005$ for DST, compared to initial data); this was expected because of the perturbation in the temporal succession of data. The median remained slightly higher than 0.5 only for SST ($h(2)_{shuf} = 0.545$) which means that still there is a persistent behavior (multifractality of type (i)) in those simple saccadic data series. In contrast, for DST ($h(2)_{shuf} = 0.505$) the shuffling procedure seems to annihilate the persistence in saccadic data (multifractality of type (ii)).

Similar results were reported by Ihlen and Vereijken (2010) demonstrating that the main Hurst exponent increases when the subjects provide faster response in a prior encoding task or that the multifractal singularity spectrum width is dependent on the interrelation between the task instruction and the changes in attention to the stimulus.

From Fig. 6b it is observed that initial SST data show higher multifractality strength (median 0.552) than DST one (median 0.267). This result shows that when adding a new task, the brain responses to the combined action/perception task, shows a reducing of the multifractality of fluctuations.

In the case of Δh for shuffled data (Fig. 6b), DST median increased from 0.267 to 0.332, while for SST, the median remained approximately the same (0.561 compared to 0.572 after shuffling). Narrow boxes can be seen after shuffling – for SST from 0.082 to 0.046 box length and for DST from 0.092 to 0.063. The intervals between box tails (practically the whole variation range) were shortened after data shuffling in both types of saccadic series, which means that multifractality strength does no vary as much as for initial data. In other words, data shuffling diminished multifractality but did not destroy it.

In all cases, we observed that histograms of the series show an approximately log-normal distribution, in agreement with the results of the study of inter-gaze distance reported by Kelty-Stephen and Mirman (2013). As illustration, Fig. 7 presents the peak speed data distributions for the subject whose time series were given in Fig. 2. The histograms are reasonably well fitted by log-normal probability distributions (continuous curves) characterized by the following parameters: Fig. 7a: mean 0.232 and standard deviation 0.016; Fig. 7c: mean 0.250 and standard deviation 0.016. The goodness of the fit is qualitatively tested by the quantile plots, a graphical method for comparing two probability distributions by plotting their quantiles against each other. As shown in Fig. 7b and d, the deviation from the ideal fit in each case (the broken lines) is small (no more than 15%), showing that the fit is reasonably good.

Log-normal type distribution in eye movement was reported by Kelty-Stephen and Mirman (2013) and Ihlen (2012) as evidence of nonlinear interactions across scales in the dynamics of visual cognition. In this context we give further support, demonstrating that also in the case of peak speed fluctuations, the dynamics is not purely stochastic but are interaction-dominant, presenting long range correlations. The processes responsible for the fluctuations are not independent and simple cumulative (like in component-dominant dynamics) but they non-linearly interact and their actions are integrated.

3.2. The Lempel–Ziv (L–Z) complexity method

To apply the L–Z complexity test, a numerical sequence of data has first to be transformed into a symbolic sequence. The usual approach is to convert the series into a sequence of only two symbols: 0 and 1. This can be carried out by comparing the data with a threshold (usually the median) and whenever the signal is larger than or equal to the threshold, the particular piece of data is replaced by 1, otherwise by 0. The next step is parsing the obtained symbolic sequence, i.e. identifying the number of distinct binary patterns present in the sequence. The complexity index is given by the number of distinct patterns contained in the sequence. Patterns or correlations in a given sequence render its complexity smaller than that of a random sequence. Details on the parsing procedure

Author's personal copy

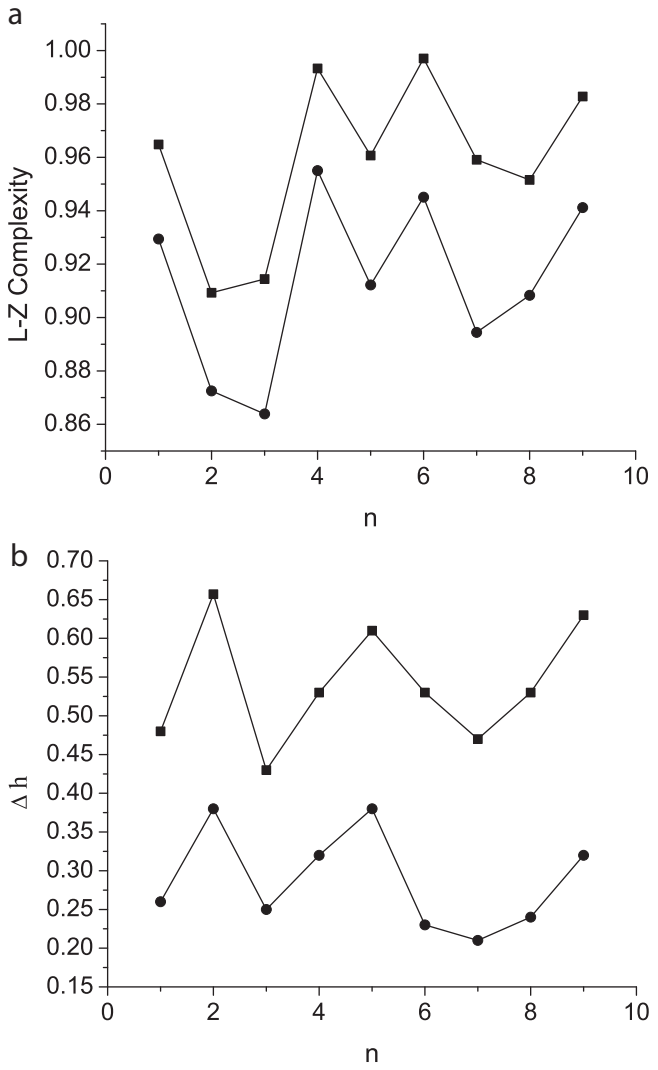

Fig. 8. (a) L–Z complexity index and (b) multifractality strength – squares for SST and circles for DST saccades for each subject; *n*-indexes the subject.

can be found in the papers of Lempel and Ziv (1976) and Hu et al. (2006).

A genuinely random string asymptotically approaches its theoretical complexity as its length n grows. It is well established that the results obtained using the L–Z complexity analysis are dependent on the characteristics of the series as well as on its length. A very complex (noise-like) experimental string with finite length usually has an L–Z complexity index slightly larger than the theoretical value 1. In computational experiments carried out on binomial data series (known as typical multifractals), we observed that for a data series of length $n = 10{,}000$ the theoretical value is obtained with very good precision. As the series analyzed in this work are not long enough to give very accurate L–Z complexity values, we used a correction method proposed by Hu et al. (2006):

$$LZ(n) = \frac{C_{LZ}(n) - C_{constLZ}(n)}{C_{randLZ}(n) - C_{constLZ}(n)} \quad (6)$$

This enables us to get reliable results from our data. Here $LZ(n)$ is the corrected value of the Lempel–Ziv index for the analyzed series, $C_{LZ}(n)$ is the Lempel–Ziv index computed according to the definition (Lempel and Ziv, 1976), $C_{constLZ}(n)$ and $C_{randLZ}(n)$ are L–Z indices for constant series, respectively a white Gaussian noise series, both with the same length n as the analyzed series. As shown by Hu et al. (2006) the corrected L–Z complexity index is almost independent of the sequence length.

The results obtained according to this procedure are shown in Fig. 8.

We observe that for all subjects, the L–Z complexity index for SST is larger than the corresponding value for DST: $LZ_{SST} > LZ_{DST}$ ($p < 0.005$). This is consistent with previous results on the multifractal analysis by supporting the diminishing of the randomness of the fluctuations in the combined action–perception task. Moreover, the L–Z index follows practically the same dependence for all subjects as the multifractality strength for the two experimental procedures (Fig. 8b). The smaller values for DST confirm a higher correlated deterministic dynamics when a combined action–perception task is involved.

As multifractal analysis investigates long range fluctuation correlations and the L–Z complexity presents the departure of a time series from randomness characteristic of Gaussian white noise, the two types of analysis offer complementary information on the dynamics of neural pathways involved in the eye movement.

Since the difference in the multifractality strength for SST and DST over the subjects is practically constant, we suggest to consider the average value of this difference as parameter to measure the action–perception interaction.

4. Conclusion

Analysis of the peak speed data of saccadic eye movements, using the MF-DFA and Lempel–Ziv complexity index, shows significantly different results in a pure action task and a combined action–perception task.

We observe that while for small fluctuations ($q < 0$) the change in $h(q)$ from SST to DST is qualitatively insignificant (describes positive correlation in both cases), for large fluctuations ($q > 0$), the change in $h(q)$ shows a transition from no correlation to positive correlation. One could conclude that the narrower range of the average Hurst exponent in DST compared to SST is the result of the subject's focusing on a more difficult task, the combined action–perception task. The smaller values of the multifractality strength for dual decision task saccades compared to simple saccadic series suggest a decreasing in the fluctuation distribution when the subject's cognitive load increased. Shuffling data showed possibly different contributions to multifractality for SST and DST saccadic movements.

Similarly, the normalized Lempel–Ziv complexity index is significantly smaller in the saccade dual decision task than in the simple one, supporting the diminishing of the randomness of the fluctuations in the combined action–perception task and suggesting a more correlated deterministic dynamics. Addition of a simple decision task implies the activation of the new network of neurons and as consequence, the effect of the nonlinear interaction modifies the multifractality of the fluctuations response in order to obtain a task optimization.

The non-linear analysis of eye speed fluctuations appears to be an efficient way to design a sensitive method for investigation of the subtle cognitive effects on eye movements in combined action–perception task. We propose to consider the average value of the difference between the vales of the multifractality strength for SST and DST as a measure of the action–perception interaction, since this difference over the subjects is practically constant. The finding that saccade peak speed has a multifractal structure potentially has important implications for how we theorize about visual control.

The underlying neural pathway is governed by processes that are regulated by complex dynamics that incorporate memory of past events. The strength of this memory, measured by the Hurst

Author's personal copy

exponent, is proved to be altered under the addition of new tasks and, as expected, is different in SST and DST because the neural dynamics is modified by the nonlinear interaction in the brain pathways for action and perception when two neural pathways are simultaneously activated.

Acknowledgement

This research was supported by FP 7 Project IRSES People 269263 “CERVISO”.

References

Aboy M, Hornero R, Abásolo D, Alvarez D. Interpretation of the Lempel–Ziv complexity measure in the context of biomedical signal analysis. IEEE Trans Biomed Eng 2006;53:2282–8.

Amigo JM, Szczepaski J, Wajnryb E, Sanchez-Vives MV. Estimating the entropy rate of spike trains via Lempel–Ziv complexity. Neural Comput 2004;16:717–36.

Astefanoaei C, Pretegiani E, Optican LM, Creanga D, Rufa A. Eye movement recording and nonlinear dynamics analysis – the case of saccades. Rom J Biophys 2013;23:81–92.

Ausloos M. Measuring complexity with multifractals in texts. Translation effects. Chaos Soliton Fract 2012;45:1349–57.

Chaitin GJ. On the length of programs for computing finite binary sequences. J ACMS 1966;13(4):547–69.

Coey CA, Wallot S, Richardson MJ, Van Orden G. On the structure of measurement noise in eye-tracking. J Eye Movement Res 2012;5:1–10.

Daye PM, Optican LM, Roze E, Gaymard B, Pouget P. Neuromimetic model of saccades for localizing deficits in an atypical eye-movement pathology. J Transl Med 2013;11:125–39.

Dojnow PD, Vitanov N. Dynamics of the multifractal measures of EEG. In: Front Hum Neurosci Proc. 10th Int Conf Cogn Neurosci; 2008.

Dutta S, Ghosh D, Shukla S, Dey S. Multifractal parameters as an indication of different physiological and pathological states of the human brain. Physica A 2014;396:155–63.

Hays A Jr, Richmond BJ, Optican LM. In: Unix-based multiple-process system, for real-time data acquisition and control; 1982.

Hu J, Gao J, Principe JC. Analysis of biomedical signals by the Lempel–Ziv complexity: the effect of finite data size. IEEE Trans Biomed Eng 2006;53:2606–9.

Ihlen EAF, Vereijken B. Interaction-dominant dynamics in human cognition: beyond $1/f$(alpha) fluctuation. J Exp Psychol Gen 2010;139:436–63.

Ihlen EAF. Introduction to multifractal detrended fluctuation analysis in Matlab. Front Physiol 2012;3(141):1–18.

Kantelhardt JW, Zschiegner SA, Koscielny-Bunde E, Havlin S, Bunde A, Stanley HE. Multifractal detrended fluctuation analysis of nonstationary time series. Physica A 2002;316:87–114.

Kelty-Stephen DG, Mirman D. Gaze fluctuations are not additively decomposable: reply to Bogartz and Staub. Cognition 2013;126:128–34.

Kelty-Stephen DG, Nixon J. Notes on a journey from symbols to multifractals. Ecol Psychol 2013;25:1–62.

Kolmogorov AN. Three approaches to the quantitative de of information. Problem Inform Transm 1965;1(1):1–7.

Kumar S, Gu L, Ghosh N, Mohanty SK. Multifractal detrended fluctuation analysis of optogenetic modulation of neural activity. In: Proc. SPIE 8586 Optogenetics: Optical Methods for Cellular Control 858608; 2013.

Leigh RJ, Kennard C. Using saccades as a research tool in the clinical neurosciences. Brain 2004;127:460–77.

Lempel A, Ziv J. On the complexity of finite sequences. IEEE Trans Inform Theory 1976;22:75–81.

Muzy F, Bacry E, Arneodo A. Multifractal formalism for fractal signals: the structure–function approach versus the wavelet transform modulus-maxima method. Phys Rev E 1993;47:875–84.

Saslow M. Effects of components of displacement-step stimuli upon latency for saccadic eye movement. J Opt Soc Am 1967;57:1024–9.

Schmeisser ET, McDonough JM, Bond M, Hislop PD, Epstein AD. Fractal analysis of eye movements during reading. Optom Vis Sci 2001;78:805–14.

Shelhamer M. Sequences of predictive saccades are correlated over a span of ~2 s and produce a fractal time series. J Neurophys 2005;93:2002–11.

Stan C, Cristescu MT, Buimaga-Iarinca L, Cristescu CP. Investigation on series of length of coding and non-coding DNA sequences of bacteria using multifractal detrended cross-correlation analysis. J Theor Biol 2013;321:54–62.

Suckling J, Wink AM, Bernard FA, Barnes A, Bullmore E. Endogenous multifractal brain dynamics are modulated by age, cholinergic blockade and cognitive performance. J Neurosci Meth 2008;174:292–300.

Szczepaski J, Amigó JM, Wajnryb E, Sanchez-Vives MV. Application of Lempel–Ziv complexity to the analysis of neural discharges. Network 2003;14:335–50.

Telesca L, Colangelo G, Lapenna V, Macchiato M. Fluctuation dynamics in geoelectrical data: an investigation by using multifractal detrended fluctuation analysis. Phys Lett A 2004;332:398–404.

Tessier Y, Lovejoy S, Hubert P, Schertzer D, Pecknold S. Multifractal analysis and modeling of rainfall and river flows and scaling, causal transfer functions. J Geophys Res 1996;31D:26427–40.

Wang J, Ning X, Chen Y. Multifractal analysis of electronic cardiogram taken from healthy and unhealthy adult subjects. Physica A 2003;323:368–561.

Wong AL, Shelhamer M. A long-memory model of motor learning in the saccadic system: a regime-switching approach. Ann Biomed Eng 2013;41:1613–24.

Yu CX, Gilmore M, Peebles WA, Rhodes TL. Structure function analysis of long-range correlations in plasma turbulence. Phys Plasmas 2003;10:2772–80.

Zheng Y, Gao J, Sanchez JC, Principe JC, Okun MS. Multiplicative multifractal modeling of human neuronal activity. Phys Lett A 2005;344:253–64.